ACS SyntheticBiology

pubs.acs.org/synthbio Research Article

Remotely Controllable Engineered Bacteria for Targeted Therapy of *Pseudomonas aeruginosa* Infection

Yanmei Gao,[⊥] Jingjing Wei,[⊥] Lu Pu, Shengwei Fu, Xiaochen Xing, Rongrong Zhang,* and Fan Jin*

Cite This: https://doi.org/10.1021/acssynbio.2c00655 Read Online

ACCESS | Metrics & More | Article Recommendations | Supporting Information

ABSTRACT: *Pseudomonas aeruginosa* (*P. aeruginosa*) infection has become an intractable problem worldwide due to the decreasing efficacy of the mainstay therapy, antibiotic treatment. Hence, exploring new drugs and therapies to address this issue is crucial. Here, we construct a chimeric pyocin (ChPy) to specifically kill *P. aeruginosa* and engineer a near-infrared (NIR) light-responsive strain to produce and deliver this drug. Our engineered bacterial strain can continuously produce ChPy in the absence of light and release it to kill *P. aeruginosa* via remotely and precisely controlled bacterial lysis induced by NIR light. We demonstrate that our engineered bacterial strain is effective in *P. aeruginosa*-infected wound therapy in the mouse model, as it eradicated PAO1 in mouse wounds and shortened the wound healing time. Our work presents a potentially spatiotemporal and noninvasively controlled therapeutic strategy of engineered bacteria for the targeted treatment of *P. aeruginosa* infections.

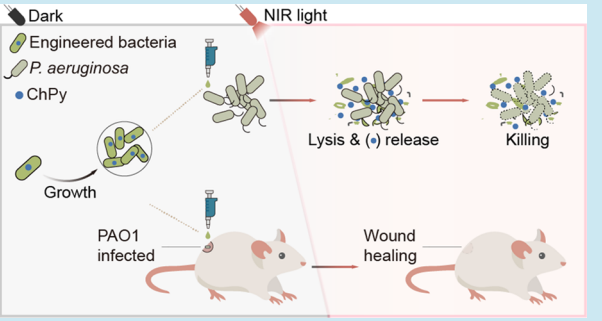

KEYWORDS: *P. aeruginosa infection, engineered bacteria, near-infrared (NIR) light, chimeric pyocin*

INTRODUCTION

Pseudomonas aeruginosa (*P. aeruginosa*) is a ubiquitous and opportunistic pathogen with strong environmental adaptability and survivability that can infect humans, animals, and plants.[1] Acute or chronic wound infections caused by *P. aeruginosa* are extremely troublesome, as *P. aeruginosa* is both intrinsically resistant to numerous antibiotics and can acquire resistance during therapy, resulting in conventional antibiotics becoming less effective or ineffective.[1] Moreover, the rate of development of new antibiotics does not match the growth of antibiotic resistance.[2] Therefore, it is necessary to address these problems with other antibacterial agents, such as organic acids,[3] antimicrobial peptides (AMPs),[4] pyocins,[5] and nanoparticles,[6,7] which reportedly kill antibiotic-resistant *P. aeruginosa* efficiently in vitro or in animal models.[8] Especially, pyocins, bacteriocins produced by certain *P. aeruginosa* strains for the rapid elimination of closely related strains, are considered to be promising alternatives or adjuncts to antibiotics for several reasons.[9] First, using pyocins to treat *P. aeruginosa* infections can help avoid dysbiosis caused by broad-spectrum antibacterial agents, as pyocins exhibit narrow-spectrum antibacterial activity.[5] Second, pyocins have been shown to be highly effective in killing *P. aeruginosa*, and no side effects have been observed in several animal models.[10−12] Third, several pyocins are suitable for protein engineering as their function domains are well-studied.[13−16] However, while using pyocins alone or in combination with antibiotics performs well both in vitro and in vivo, their performance in clinical trials is limited due to potential degradation and inactivation in body fluids.[15] Nevertheless, this issue could be circumvented or alleviated by utilizing an appropriate drug delivery system.

Engineered bacteria have emerged as an ideal drug delivery system due to their incomparable advantages over conventional therapeutic strategies.[17] Researchers can rationally design and construct a variety of multifunctional engineered bacteria using synthetic biological tools.[14,18−22] Most importantly, engineered bacteria can deliver drugs to specific sites in the body that are difficult to reach via parenteral or oral drug delivery.[17,23] Currently, several *Escherichia coli* (*E. coli*) strains had been engineered for the treatment and prevention of *P. aeruginosa* infections, in which the engineered strains produce and deliver pyocins or AMPs in response to *P. aeruginosa*-specific quorum sensing (QS) molecules, acyl-homoserine lactones (AHLs).[14,19,21,22] However, the antimicrobial activities of these engineered bacteria were greatly limited by their dependence on the surrounding *P. aeruginosa* density and their ability to detect AHL.[21,24] Additionally, there were very limited experimental data on the effectiveness of these therapies in vivo.[14,19,21,22] Thus, in this study, we aimed to construct an

Received: December 6, 2022

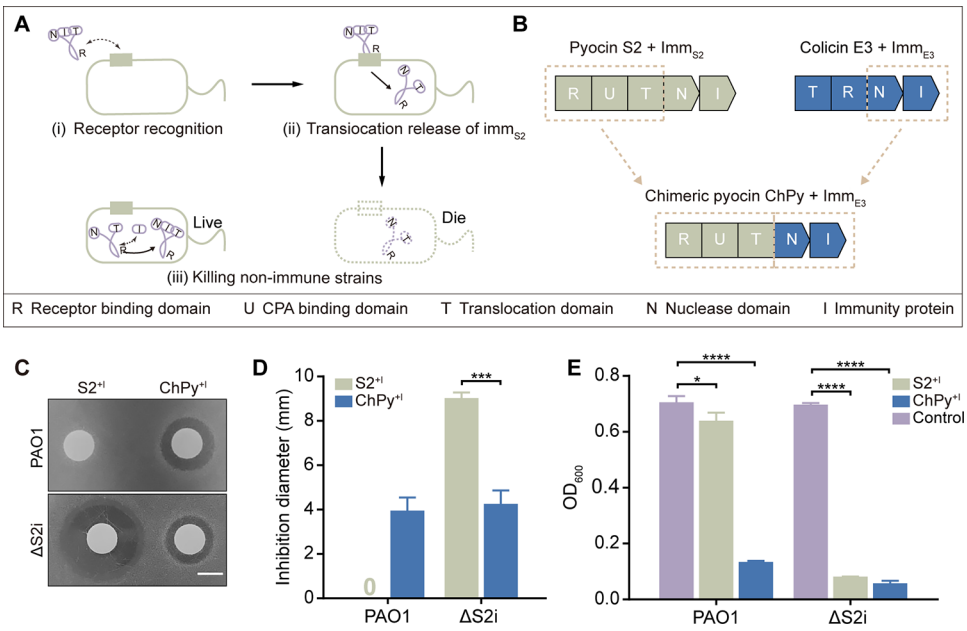

Figure 1. Structural domains of chimeric pyocin ChPy and its anti-*P. aeruginosa* ability assay. (A) Schematic of the main mechanism of action of pyocin S2^{+I} complexes. CPA, common polysaccharide antigen. (B) Protein domain architecture of pyocin S2, colicin E3, and chimeric pyocin ChPy and their corresponding immune proteins. (C) Pyocin complex S2^{+I} and ChPy^{+I} sensitivity of wild-type *P. aeruginosa* PAO1 and its variant strain ΔS2i on the 1.5% FAB agar. Scale bar = 5 mm. (D) Diameters of the inhibition zones formed in panel (C), where 0 means no inhibition circle was observed. (E) OD$_{600}$ values of PAO1 and ΔS2i after 13 h of coincubation with purified complexes S2^{+I} and ChPy^{+I} and the dialysate (control). S2^{+I} and ChPy^{+I} represent the 1:1 complexes formed by pyocin S2 and ChPy with their corresponding immune proteins, respectively. In (D) and (E), error bars represent means ± s.d., $n = 3$, $^{*}P \leq 0.05$, $^{***}P \leq 0.001$, $^{****}P \leq 0.0001$ (Student's *t*-test).

engineered bacterial strain that can be remotely and precisely controlled for targeted treatment of *P. aeruginosa* infection and to evaluate its efficacy in vivo.

Precisely triggering the release of antimicrobial drugs can maximize therapeutic efficacy and reduce the adverse effects of engineered bacteria. However, traditional chemical inducers are often environmentally dependent and not easily removed.[25] In contrast, light, characterized by time- and space-independent, orthogonal, and noninvasive input, holds the promise for more precise control of engineered bacterial systems.[25,26] Particularly, near-infrared (NIR) light is considered to be an ideal tool for modulating engineered bacteria in living mammals due to its low phototoxicity and deep tissue penetration.[27,28] We previously demonstrated that the engineered strain Q017 was capable of lysing in response to NIR light. The delivery system of this strain can assist us in achieving precise control of drug release remotely with NIR light.

In this paper, for *P. aeruginosa*-specific killing, we designed and constructed a chimeric pyocin ChPy. Furthermore, we programmed the genetic circuit of the Q017 strain to continuously produce ChPy during its growth. We demonstrated that our engineered bacteria retained the ability to lyse in response to NIR light and showed high in vitro anti-*P. aeruginosa* activity after NIR light-induced bacterial lysis. Additionally, we found that our engineered bacterial strain was effective in reducing *P. aeruginosa* infection in the PAO1-infected mouse wound model, as evidenced by the eradication of *P. aeruginosa* in the wounds and acceleration of wound healing.

RESULTS

Novel Chimeric Pyocin ChPy Specifically Kills *P. aeruginosa* Strains Both Sensitive and Resistant to Pyocin S2. Pyocin S2, produced by most clinical isolates of *P. aeruginosa* strains, reportedly kills nonimmune *P. aeruginosa* strains efficiently and specifically.[11,29] It has four well-studied function domains, each responsible for its targeted anti-*P. aeruginosa* process:[30−33] the common polysaccharide antigen (CPA) binding domain (U) assists pyocin S2 in concentrating on the bacterial surface, where it further binds to bacterial surface-specific receptors via the receptor binding domain (R); then, the translocation domains (T) translocate it across the bacterial outer membrane; finally, it kills nonimmune strains by degrading their DNA via the nuclease domain (N) (Figure 1A). For pyocin S2 producers, they protect themselves from the toxicity of endogenous or exogenous pyocin S2 by expressing excess immune protein, Imm$_{S2}$, to form tight 1:1 complexes S2^{+I} (S2+Imm$_{S2}$) with pyocin S2.[30,31] Namely, although some *P. aeruginosa* strains can transfer pyocin S2 into their cytoplasm, they grow normally as they contain the pyocin S2 immunity gene. Thus, to address this issue, we fused a chimeric pyocin ChPy by replacing the nuclease domain and immune protein of pyocin S2 with those of colicin E3, a well-known bacteriocin produced by *E. coli*[34] (Figure 1B). *P. aeruginosa* cannot possess protein Imm$_{E3}$ as it derived from *E. coli*. Hence, we deduced that chimeric pyocin ChPy can specifically kill *P. aeruginosa* strains immune and nonimmune to pyocin S2.

To prove our conjecture, we induced and purified S2^{+I} and ChPy^{+I} (ChPy+Imm$_{E3}$) complexes, respectively (detailed description in the Methods). Two proteins of S2 (73.9 kDa) and ChPy (71.1 kDa) were detected on SDS-PAGE gel (Figure S1A). We first evaluated the toxicity of the purified

https://doi.org/10.1021/acssynbio.2c00655
ACS Synth. Biol. XXXX, XXX, XXX−XXX

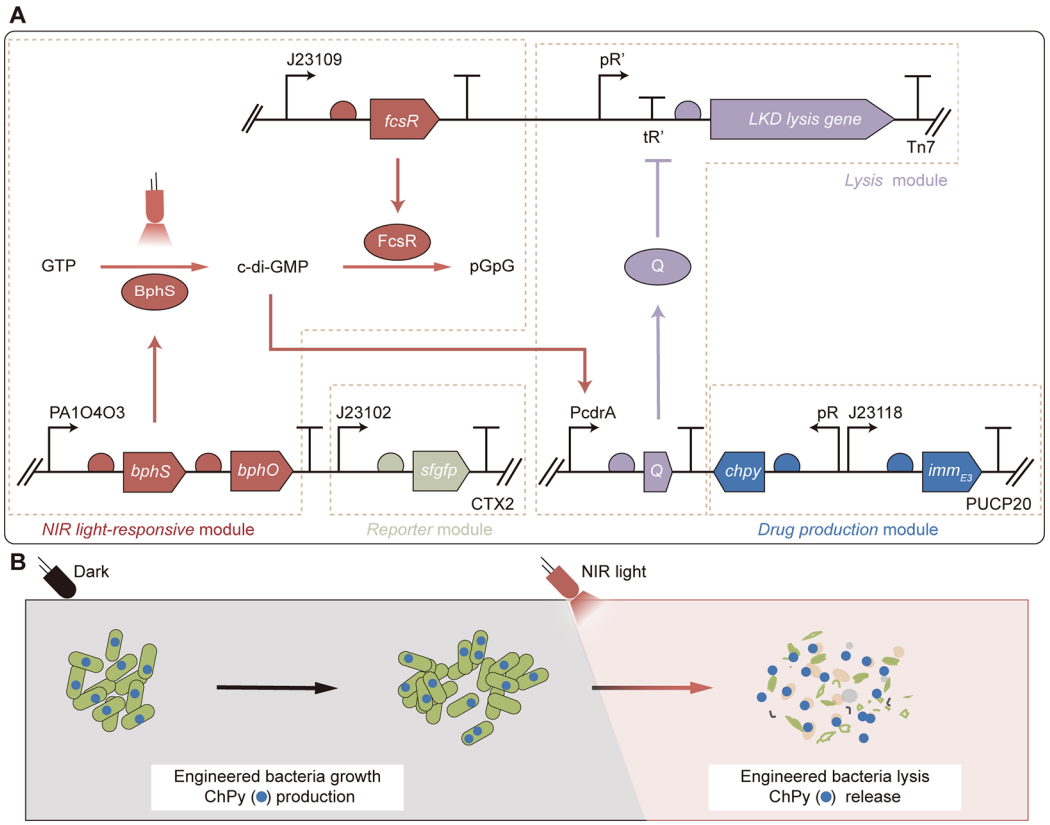

Figure 2. Detailed gene circuit diagram of engineered bacteria and the near-infrared (NIR) light-modulated anti-*P. aeruginosa* process. (A) Detailed gene circuit diagram of the engineered bacteria. Tn7 and CTX2 denote attTn7 and ϕCTX sites in the bacterial chromosome, respectively; PUCP20 is the plasmid vector name. (B) Schematic diagram of NIR light-modulated drug release of engineered bacteria.

complexes ($S2^{+I}$ and $ChPy^{+I}$, 0.158 mg/mL) against both *P. aeruginosa* and *E. coli*. We found that the chimeric pyocin ChPy, like pyocin S2, specifically killed *P. aeruginosa* strains (Figure S1B). Subsequently, we compared the toxicity of $S2^{+I}$ and $ChPy^{+I}$ against both the wild-type PAO1 and its variant strain ΔS2i (knockout pyocin S2 and Imm_{S2} protein gene). The results showed that $ChPy^{+I}$ formed inhibitory zones of 3.957 and 4.255 mm diameters on FAB agar plates containing wild-type PAO1 (PAO1 plate) and ΔS2i (ΔS2i plate), respectively (Figure 1C,D). In contrast, $S2^{+I}$ only formed an inhibitory zone of 9.031 mm diameter on the ΔS2i plate (Figure 1C,D). That is to say, ChPy could kill the *P. aeruginosa* strains immune and nonimmune to pyocin S2. This result was confirmed in bacterial liquid culture by monitoring the OD_{600} values of strains PAO1 and ΔS2i mixed with purified $S2^{+I}$ and $ChPy^{+I}$ (0.035 mg/mL), respectively (Figure 1E). Overall, we conclude that the chimeric pyocin ChPy can specifically kill *P. aeruginosa* strains regardless of whether they possess the pyocin S2 immunity gene, as expected.

Design of the Genetic Circuit for the NIR Light-Modulated Drug Delivery System. To develop a precisely and remotely controllable therapy for specifically treating *P. aeruginosa* infections, we engineered an attenuated strain of the wild-type *P. aeruginosa* PAO1 strain, ExoST, to produce chimeric pyocin ChPy in the dark and kill *P. aeruginosa* by releasing ChPy through bacterial lysis in response to NIR light (Figure 2B). The detailed genetic circuit of the engineered bacteria is shown in Figure 2A. To produce chimeric pyocin ChPy at high levels and avoid toxicity to the producer, we chose different constitutive promoters to express ChPy and its immune protein, Imm_{E3} (drug production module). The release of the chimeric pyocin ChPy was remotely and precisely regulated through the NIR light-responsive, *c*-di-GMP-mediated bacterial lysis system:[35] briefly, the phosphodiesterase, FscR, will hydrolyze the intracellular *c*-di-GMP into pGpG, maintaining a bare level of intracellular *c*-di-GMP in the dark. Upon NIR light irradiation, the *c*-di-GMP synthase BphS will be activated and synthesize two molecules of GTP into *c*-di-GMP. At this time, the rate of intracellular *c*-di-GMP synthesis exceeds that of hydrolysis, resulting in an increase in the concentration of *c*-di-GMP within the bacterial cell (NIR light-responsive module). When the intracellular *c*-di-GMP level reaches a certain threshold, the promoter PcdrA will be activated, initiating the transcription of the antitermination protein Q. This protein functions as a transcriptional antiterminator of phage λ[36] and is required for the expression of LKD lysis proteins under the control of the promoter pR'-tR'. LKD lysis proteins are capable of penetrating the membrane of the engineered bacteria, causing bacterial lysis and the subsequent release of ChPy to kill *P. aeruginosa* (lysis modules). For imaging our engineered bacteria under the microscope, we inserted a superfolder green fluorescent protein (sfGFP) into the ϕCTX site of the bacterial chromosome (reporter module). Hence, we hypothesized that the final system could enable spatiotemporal and noninvasive controlled drug delivery via NIR light for the treatment of *P. aeruginosa* infections. Figure S2 shows the genetic circuit of the host strain ExoST and the plasmid map of the final system.

https://doi.org/10.1021/acssynbio.2c00655
ACS Synth. Biol. XXXX, XXX, XXX−XXX

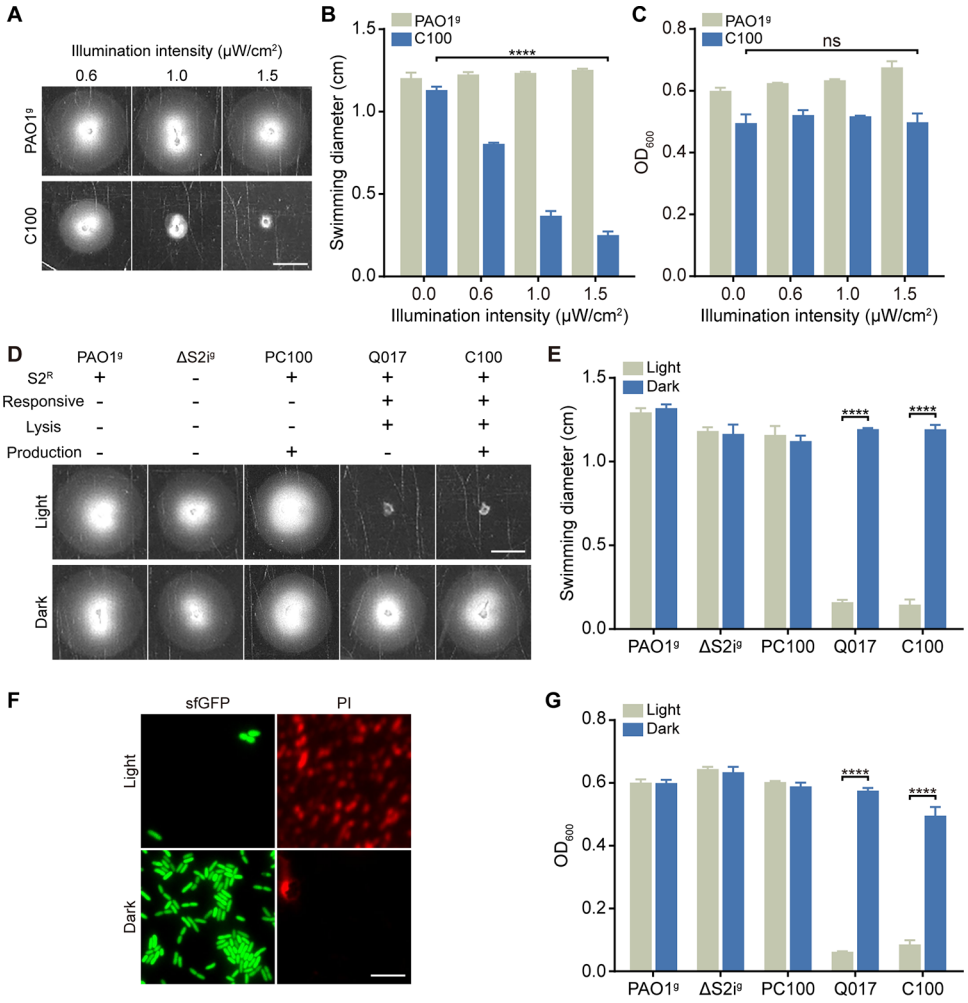

Figure 3. NIR light-activated, *c*-di-GMP-mediated assessment of the engineered bacterial lysis ability. (A) Pictures of swimming zones of strains PAO1^g and C100 on semisolid agar swimming motility plates under 0.6, 1.0, and 1.5 μW/cm^2 light intensities. Scale bar = 5 mm. Swimming zone diameters (B) and OD_{600} values (C) of PAO1^g and C100 strains under 0−1.5 μW/cm^2 light intensity. (D) Pictures of swimming zones of strains PAO1^g, ΔS2i^g, PC100, Q017, and C100 on semisolid agar swimming motility plates. Scale bar = 5 mm. Responsive, lysis, and production represent the NIR light-responsive, lysis, and drug production modules, respectively; S2^R indicates resistance to pyocin S2; + and − indicate the presence and absence of the corresponding modules within the tested strains, respectively. (E) Swimming zone diameters of panel (D). (F) Fluorescence images of strain C100; after 1 h of incubation in light or darkness, following propidium iodide (PI) dye staining, live cells (green) can express sfGFP, while dead cells (red) were stained with the PI dye. Scale bar = 5 μm. (G) OD_{600} values of strains PAO1^g, ΔS2i^g, PC100, Q017, and C100 after 13 h of incubation with and without light. In (D), (E), (F), and G, the light intensities under light conditions were 50 μW/cm^2. In (B), (C), (E), and (G), error bars represent means ± s.d., n = 3. ns = not significant, ****$P \leq 0.0001$ (Student's t-test).

Remote Manipulation of *c*-di-GMP-Mediated Lysis of the Engineered Bacteria by NIR Light. As mentioned earlier, the intracellular *c*-di-GMP level controlled by NIR light is critical in determining the lysis behavior of our engineered bacteria (Figure 2A). The swimming motility assay had been reported as a rapid method to estimate the intracellular *c*-di-GMP level.[37] Therefore, we constructed an initial version of the engineered strain (C100) containing all genetic modules and preliminarily investigated its intracellular *c*-di-GMP level under different NIR light intensities via the swimming motility assay (detailed description in the Methods). The following strains were used as controls: PAO1^g (gentamicin-resistant PAO1 strain and pyocin S2-resistant strain), ΔS2i^g (gentamicin-resistant ΔS2i strain and pyocin S2-sensitive strain), PC100 (drug production module only), and Q017 (NIR light-responsive and lysis modules only). The results indicate that only the swimming motilities of C100 and Q017 decreased with increasing NIR light intensity (Figure 3A and Figure S3A). Moreover, the intracellular *c*-di-GMP levels of our engineered strain C100 were extremely sensitive to NIR light, as the diameter of its swimming zone in the dark was 4.503 times larger than its diameter under NIR light (1.5 μW/cm^2) (Figure 3A,B), while its growth was almost unaffected (Figure 3C). The swimming motilities of C100 and Q017 strains were slightly weaker than that of PAO1^g in the dark (Figure S3A). Notably, the swimming motilities of the engineered strains C100 and Q017 were barely observed at light intensities higher than 20 μW/cm^2. The swimming zones of C100 and Q017 under NIR light (50 μW/cm^2) were much smaller than their swimming zones in the dark (3.5- and 3.1-fold in diameter) (Figure 3D,E).

To further explore the NIR light-activated, *c*-di-GMP-mediated bacterial lysis of our engineered bacteria, we measured the OD_{600} values of C100 and its control strains after incubating them under various illumination intensities. Our results showed that all strains grew normally in the dark

https://doi.org/10.1021/acssynbio.2c00655
ACS Synth. Biol. XXXX, XXX, XXX−XXX

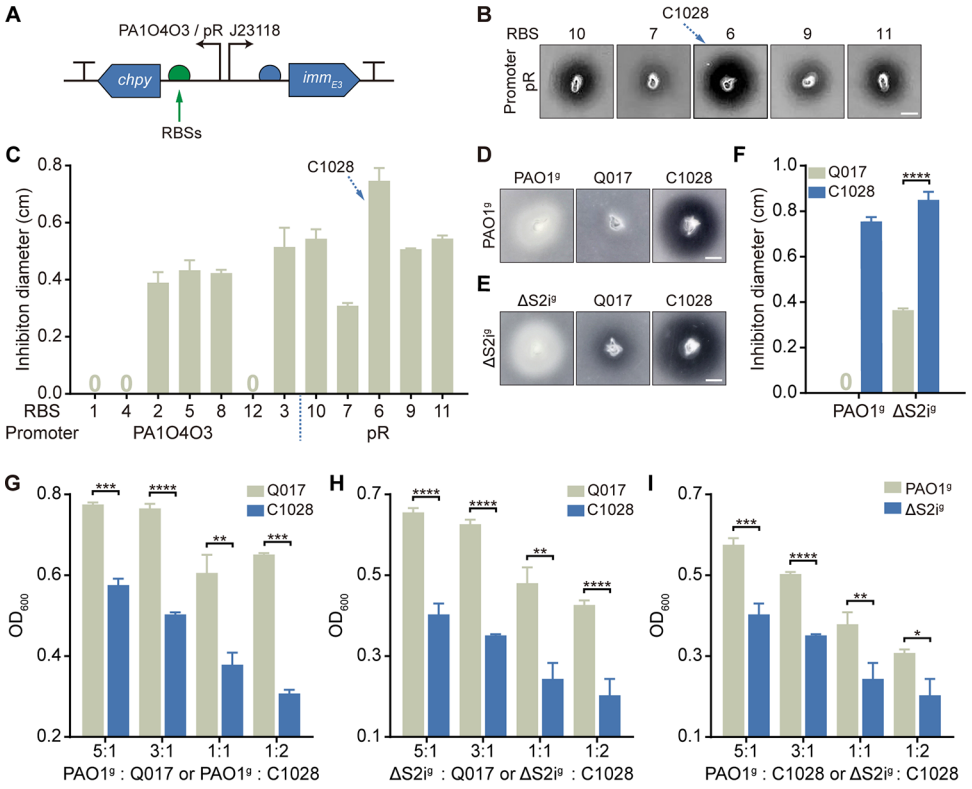

Figure 4. In vitro anti-*P. aeruginosa* functional assays of the engineered bacteria. (A) Schematic diagram of the drug production module, where ChPy protein expression levels were altered by using different intensities of RBSs (green arrows) and promoters (PA1O4O3 or pR). (B) Images of the inhibition zones formed on PAO1^g plates by engineered bacteria under NIR light, where the antimicrobial abilities were determined by the promoter pR and different RBS that control ChPy expression, scale bar = 3 mm. C. Inhibition diameters of engineered bacteria with various ChPy protein expression levels on the PAO1^g plates, where 0 means no observed inhibition zone. Picture of inhibition zones formed by strains Q017 and C1028 after incubation on PAO1^g (D) and ΔS2i^g (E) plates for 20 h under NIR light, where strains PAO1^g and ΔS2i^g were used as controls, scale bar = 2 mm. (F) Inhibition diameters of panels (D) and (E), where 0 means no observed inhibition zone. OD_{600} values of PAO1^g (G) and ΔS2i^g (H) coculture with strains Q017 and C1028 at different volume ratios under NIR light for 23 h. (I) OD_{600} values of PAO1^g and ΔS2i^g coculture with strains C1028 at different volume ratios under NIR light for 23 h. If NIR light illumination was required, the light intensity was 50 $\mu W/cm^2$. In (C), (F), (G), (H), and (I), error bars represent means ± s.d., $n = 3$, $^*P \leq 0.05$, $^{**}P \leq 0.01$, $^{***}P \leq 0.001$, $^{****}P \leq 0.0001$ (Student's *t*-test).

(Figure S3B), while only the OD_{600} values of C100 and Q017 decreased with increasing NIR light intensity (Figure S3C). Under dark conditions, the OD_{600} values of C100 and Q017 were 10.7 and 8.11 times higher, respectively, than those of the two strains under NIR light at an intensity of 50 $\mu W/cm^2$ (Figure 3G). Finally, we confirmed that the decrease in OD_{600} values of the engineered bacteria under NIR light was due to the NIR light-activated, *c*-di-GMP-mediated bacterial lysis by utilizing the propidium iodide (PI) staining assay to determine bacterial viability and assess cell membrane integrity (Figure 3F and Figure S3D).

Taken together, these results suggest that the intracellular *c*-di-GMP level of our engineered bacteria is low under dark conditions and raises in response to NIR light, which inhibits bacterial swimming motility and triggers bacterial lysis. This process causes the engineered bacteria to appear trapped in the stabbing position of the semisolid agar motility plate (Figure 3D). Namely, our engineered bacteria can grow normally in the dark, and their lysis can be precisely controlled by NIR light, as hypothesized. The NIR light intensity used in the remainder of this paper is 50 $\mu W/cm^2$ unless otherwise stated.

Engineered Bacterial Strain C1028 Shows High Anti-*P. aeruginosa* Activity In Vitro. To further evaluate the antibacterial ability of our engineered strain C100, we stabbed it into semisolid agar motility plates containing PAO1^g (PAO1^g plate) (detailed description in the Methods). The diameter of the inhibition zone formed after its lysis in PAO1^g plates then can represent its anti-*P. aeruginosa* ability as we showed earlier that it lysed without observable swimming movements in the semisolid agar motility plates under NIR light (Figure 3D,F). However, the strain C100 showed a negligible anti-*P. aeruginosa* effect (Figure S4A). We subsequently confirmed that the low antimicrobial activity of the C100 strain was caused by insufficient expression of ChPy in this strain, through the fusion of the cyOFP1 fluorescent protein to the C-terminus of the ChPy protein (Figure S5A–D).[38,39] Thus, to increase the ChPy expression, we designed a series of ribosomal binding sites (RBS) with high predicting translation initiation efficiency through the RBS calculator (Table S1)[40] and used them to replace the original RBS upstream of the chpy gene in the strain C100 (Figure S4A). Although the antibacterial activity of the new strain C300 is significantly improved compared to that of the C100 strain, it is still not strong enough (Figure S4A). Further analysis revealed that the PA1O4O3 promoter, which contains the repetitive sequence (two laco sites), was mutated when a high-strength RBS was utilized. Therefore, we replaced the PA1O4O3 promoter with pR in front of protein ChPy and subsequently redesigned several RBSs (Table S1) to optimize the ChPy expression (Figure S4B).[40] Our results showed that the combination of

https://doi.org/10.1021/acssynbio.2c00655
ACS Synth. Biol. XXXX, XXX, XXX−XXX

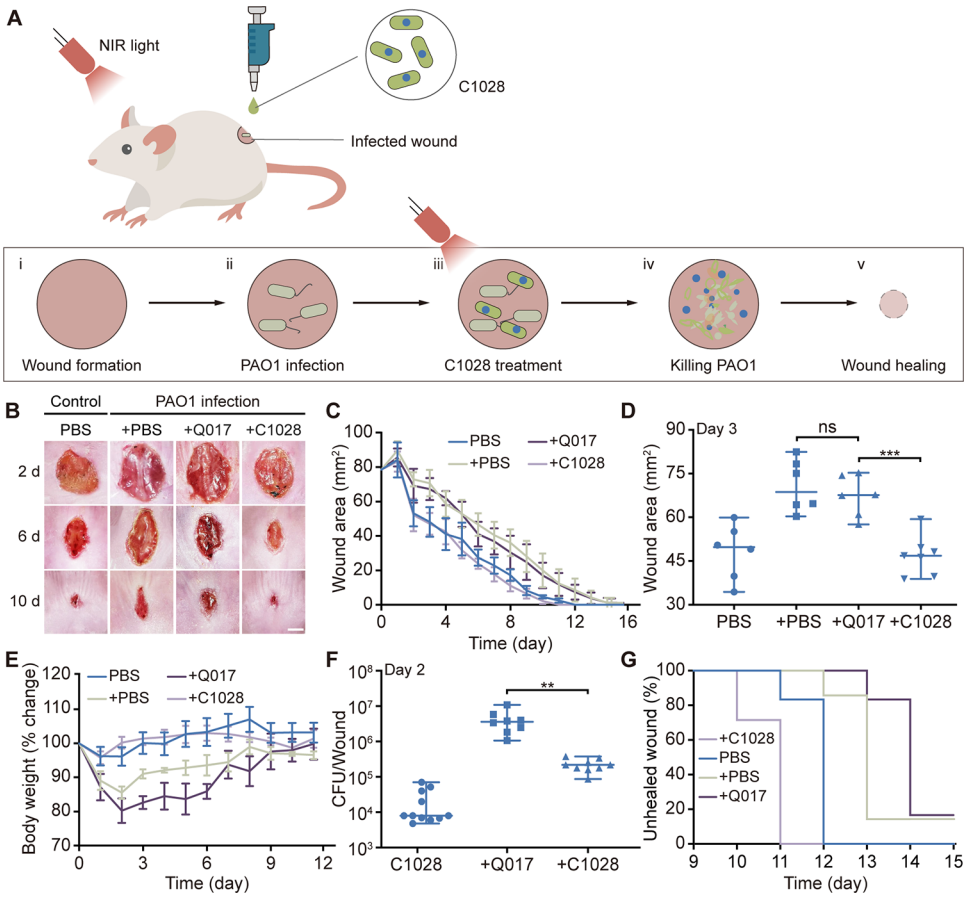

Figure 5. Assessment of the therapeutic ability of the strain C1028 in the PAO1-infected mouse wound model. (A) Procedure of establishing PAO1-infected wound models on mice and the corresponding antibacterial therapy of the strain C1028. (B−E) Experimental results of mice after different treatments (PBS, +PBS, +Q017, and +C1028). (B) Photographs at 2, 6, and 10 days. Scale bar = 3 mm. (C) Wound area within 15 days, (D) wound area on day 3, and (E) body weight change within 11 days (%). F. Colony-forming units (CFU) of mice after different treatments (C1028, +Q017, and +C1028) on day 2. (G) Proportion of mice in the PBS, +PBS, +Q017, and +C1028 groups with unhealed wounds between 9 and 15 days. Error bars represent means ± s.d., n = 6−11, ns = not significant, $^{**}P \leq 0.01$, $^{***}P \leq 0.001$ (Student's t-test).

pR (promoter) and RBS6 (optimized RBS, predicted strength of 1028) generated the highest antibacterial activity, and we named this strain C1028 (Figure 4B,C and Figure S4B). Notably, all test strains engineered in this study displayed minor inhibition zones on the PAO1^{g} plate in the absence of light. This is because our host strain has the ability to autonomously secrete pyocins into the extracellular space (Figure S4A,B).[41−43] Subsequent experiments showed a positive correlation between the diameter of the inhibition zones formed by our test engineered strains on PAO1^{g} plates and their intracellular ChPy expression (Figure S5G). Notably, the expression level of ChPy protein in the C1028 strain was significantly higher than that observed in other strains (Figure S5D−F). Namely, it is reasonable for us to improve the antibacterial activity of engineered bacteria by optimizing the expression of ChPy (Figure 4A).

Subsequently, we evaluated the anti-*P. aeruginosa* activities of strain C1028 on both ΔS2i^{g} and PAO1^{g} plates under NIR light. As expected, C1028 was able to form inhibition zones on both PAO1^{g} and ΔS2i^{g} plates (Figure 4D,E). Owing to the presence of pyocin S2 in the genome of our host bacteria ExoST (Figure S6A,B), C1028 exhibited superior antibacterial activity against the ΔS2^{g} strain compared to PAO1^{g}, while the strain Q017 was only able to form an inhibition circle on ΔS2i^{g} plates (Figure 4D−F). On the ΔS2i^{g} plate, the diameter of the inhibition zone produced by the C1028 strain was 2.3 times greater than that observed with the strain Q017 (Figure 4F). Therefore, we can conclude that the drug production module plays a critical role in enhancing the antibacterial activity of our engineered bacteria.

To quantify the antibacterial ability of our engineered strain C1028 after lysis, we monitored the growth of PAO1^{g} and ΔS2i^{g} strains when cocultured with C1028 and Q017 under NIR light at volume ratios of 5:1, 3:1, 1:1, and 1:2 (detailed description in the Methods). The antibacterial activity of C1028 against *P. aeruginosa* strains increased with increasing cell numbers and varied among different strains (Figure 4G−I).

In summary, these results indicate that our engineered strain C1028 can efficiently eradicate both *P. aeruginosa* strains immune and nonimmune to pyocin S2 through NIR light-induced bacterial lysis and drug release.

Engineered Bacterial Strain C1028 Accelerates PAO1-Infected Wound Healing in a Mouse Model. To evaluate the therapeutic efficacy of the strain C1028 on *P. aeruginosa*-infected wounds, we established a mouse model with PAO1-infected wounds on the dorsal skin (Figure 5A). Prior to evaluating its therapeutic efficacy, we conducted safety assessments on the direct application of the C1028 strain to PAO1-infected wounds (C1028 group). The results indicated

https://doi.org/10.1021/acssynbio.2c00655
ACS Synth. Biol. XXXX, XXX, XXX−XXX

that the body weight change of mice in the C1028 group was more similar to that of the infected mice (PAO1 group) (Figure S7C), and the wound area of mice in the C1028 group was consistently smaller than that of mice in the uninfected group (PBS group) (Figure S7A,C). Particularly, two days after inoculation, the wound areas of mice in the C1028 group were significantly smaller than those of mice in the PBS group (Figure S7B) ($P = 0.0076$), which suggests that the reduction may be attributed to immune responses stimulated by the strain C1028 or its lysates.[44]

Subsequently, to assess the potential of engineered bacteria C1028 as a therapeutic agent for PAO1-infected wounds, we divided mice with wounds into five groups based on the subsequent treatments: an uninfected control group treated with sterile PBS (PBS), a PAO1-infected group treated with sterile PBS buffer (+PBS), a PAO1-infected group treated with the Q017 strain (+Q017), a PAO1-infected group treated with the C1028 strain and with NIR illumination (+C1028), and a PAO1-infected group treated with the C1028 strain without NIR illumination (+C1028^{d}) (detailed description in the Methods). The wound area of the +C1028^{d} group was not significantly different from that of the +PBS group within 3 days, and both were significantly larger than that of the +C1028 group (Figure S8A,B). Starting from day 4, wound healing in the +C1028^{d} group became progressively faster than that in the +PBS group, ultimately resulting in a shorter wound healing time in the +C1028^{d} group compared to the +PBS group (Figure S8A). Similarly, the weight loss of mice in the +C1028^{d} group was intermediate between that of the +C1028 and +PBS groups within 3 days but began to rebound significantly from day 4 (Figure S8C). We hypothesized that light exposure during the daily measurement of the mouse weight and wound area might have caused the lysis of some of our engineered bacteria, leading to changes in the parameters of the +C1028^{d} group from day 4 onward.

Therefore, we shifted our focus to the other groups. Our findings demonstrated that the wound areas of mice in the +C1028 group were similar to those of the PBS group and consistently smaller than those of the +PBS and +Q017 groups during the same treatment period (Figure 5B,C). On day 3, the wound area of mice in the +C1028 group was already 30% smaller than that of the control group +Q017 ($P = 0.0003$), while no significant difference was observed between the wound areas of the +Q017 and +PBS groups ($P = 0.457$) (Figure 5D). These results suggest that our engineered strain C1028 is highly effective in treating PAO1-infected wounds, and its therapeutic efficacy comes from the release of targeted anti-*P. aeruginosa* drugs ChPy rather than bacterial lysates. More importantly, our findings once again confirmed the therapeutic efficacy of using C1028 to treat *P. aeruginosa*-infected wounds, as only the +PBS and +Q017 groups exhibited a significant weight loss (Figure 5E). Finally, using colony-forming unit (CFU) analysis and counting the percentage of unhealed wounds in the four mouse groups within 9−15 days, we demonstrated that the strain C1028 cleared 95% of the PAO1 strain from wounds within 2 days (Figure 5F) and accelerated wound healing by at least 2 days compared to the +PBS and +Q017 groups (Figure 5G).

These findings suggest that the engineered bacterial strain C1028 is effective in eradicating *P. aeruginosa* from wounds and accelerating wound healing in the PAO1-infected mouse wound model.

DISCUSSION

In this study, we designed and constructed a chimeric pyocin ChPy to specifically kill *P. aeruginosa* strains with or without the pyocin S2 immunity gene. Subsequently, we developed an NIR light-responsive engineered strain to produce and remotely controllably deliver the chimeric pyocin ChPy: our engineered strain, C1028, could produce ChPy under dark conditions and lyse to release the drug to specifically kill *P. aeruginosa* upon exposure to NIR light. Finally, in a PAO1-infected mouse wound model, our engineered bacteria demonstrated effectiveness in eradicating *P. aeruginosa* from the wounds and reducing the wound healing time by at least 2 days.

Broad-spectrum antibacterial drugs perhaps alter a healthy human microbiome[19] and then cause allergic reactions or other diseases.[9,45] Moreover, antibiotic overuse is a major contributing factor to the rapid increase of multidrug-resistant (MDR) pathogenic bacteria, such as *P. aeruginosa*.[46] Hence, developing and using new antibacterial drugs, especially targeted anti-*P. aeruginosa* drugs, to replace or reduce broad-spectrum antibiotics use are essential. S-type pyocins are ideal toxins as they specifically kill *P. aeruginosa*. For instance, purified pyocin S2 and S5 demonstrated superior antibacterial activity than antibiotics when employed to treat clinical isolates of *P. aeruginosa*, and no untoward effects were observed in animal models.[11,29] Moreover, given that the functional domains of some S-type pyocins are well-studied, S-type pyocin derivatives can be artificially constructed, further enriching the library of targeted anti-*P. aeruginosa* drugs.[13,14] The results of our study demonstrated that our chimeric pyocin, ChPy, can specifically kill *P. aeruginosa* strains immune and nonimmune to pyocin S2 (Figure 1C,E). Additionally, our engineered bacteria C1028 can also efficiently kill gentamicin-resistant *P. aeruginosa* strains with and without the pyocin S2 immunity gene (Figure 4D−I). Although we did not further test the antibacterial efficacy of protein ChPy or the strain C1028 against MDR *P. aeruginosa*, it is reasonable to assume that the C1028 strain has potential therapeutic utility against MDR *P. aeruginosa* based on the antimicrobial mechanism of pyocin S2 and several previous studies.[11,29,47] It should be noted that as the C1028 strain kills *P. aeruginosa* via the FpvAI receptor, it is not effective against strains lacking this receptor. Nevertheless, this gap could be filled by making engineered bacterial cocktails like phage cocktails.[48]

The precise regulation of drug delivery systems can improve therapeutic efficiency while reducing adverse effects. In the previously published studies of bacterial-based therapies for *P. aeruginosa* infection, all drug synthesis and release from engineered bacteria were regulated by the *P. aeruginosa* QS signaling molecule AHL.[14,19,21,22] Activation of the antimicrobial activity of these engineered bacteria does not require the additional inducers, enabling spontaneous response and autonomous induction in the treatment of *P. aeruginosa* infections. However, this QS-dependent induction system would be limited by both the cell density of *P. aeruginosa* surrounding the engineered bacteria and the ability of the engineered bacteria themselves to detect the signaling molecule AHL.[24] In contrast, the noninvasive inducer NIR light offers several advantages over traditional inducers. NIR light is highly controllable due to its adjustable intensity, excellent spatial and temporal resolution, low cytotoxicity, deep tissue penetration, and high robustness in complex

https://doi.org/10.1021/acssynbio.2c00655
ACS Synth. Biol. XXXX, XXX, XXX−XXX

biological environments.[49] Therefore, for the treatment of pathogenic bacterial infections, utilizing NIR light to regulate the antimicrobial activity of the engineered bacteria is a more practical and promising approach for in vivo applications. Our NIR light-responsive drug delivery systems can be remotely and precisely regulated, accelerating the development of bacterial-based therapeutics for treating pathogenic bacterial infections in clinical applications.

With the rapid development of science and technology, researchers can rationally design and utilize pathogenic bacteria and viruses to treat and prevent certain diseases. Live vaccines, for instance, stimulate the host immune system by introducing the appropriate amount of attenuated strains, thereby building immunity to the troublesome disease.[50] The widespread application of live vaccines has helped humans overcome smallpox and has significantly reduced the occurrence of diseases like mumps, measles, rubella, and rotavirus.[50] In addition to its use as a live vaccine, *Salmonella* has been proven to be the most effective bacteria for bacterial-mediated cancer therapy.[51−53] Furthermore, *Salmonella*-based cancer therapies have already been tested in a few human clinical trials.[54] In our research, although our host strain ExoST[35] is an attenuated strain of wild-type *P. aeruginosa* PAO1 (genomic knockout of *exoS*, *exoT*, and *vfr* genes), we did not observe that our engineered strain C1028 itself or its lysates delayed wound healing and reduced body weight in the mouse model (Figure 5 and Figure S7). Particularly, we treated both PAO1-infected and uninfected wounds with the strain C1028 and found that the wounds healed faster than those in the uninfected group (Figure 5D,G and Figure S5B), which may be associated with the immune response.[44] However, further experimental investigations are still required to decrease the virulence of the ExoST strain and to evaluate the safety of attenuated strains. We believe that the application of attenuated pathogens to treat pathogenic infections may lead to some unexpected surprises.

Animal models are critical for conducting fundamental research and developing therapeutics to treat wound infections. In our PAO1-infected mouse wound model, we demonstrated that our engineered strain C1028 could effectively decrease the PAO1 load in the wounds and accelerate wound healing (Figure 5F,G). However, we must acknowledge that wound infection is a complex process, with the degree of severity ranging from self-healing to life-threatening.[55] The severity of infection in our mouse model did not pose a risk to the lives of the mice. Moreover, wounds in rodents healed mainly by contraction, while wounds in humans healed by re-epithelialization and granulation tissue growth.[56] Thus, additional animal models are needed to corroborate the therapeutic effects of the engineered bacteria. However, based on the principles of engineered bacterial-based therapy and the promising preliminary experimental results, our engineered strain holds great potential as a therapeutic approach for preventing and treating *P. aeruginosa* infections.

Overall, we have constructed and demonstrated the feasibility of using NIR light-responsive engineered bacteria for treating *P. aeruginosa*-infected wounds in our preliminary study. Our study proposes a novel concept for treating pathogenic bacterial wound infections using bacterial-based therapies. Although there is still a long road ahead, we firmly believe that with the iterative optimization of our engineered strain, it will eventually become an option for clinical treatments of MDR *P. aeruginosa* infections.

METHODS

The bacterial strains and plasmids used in this study are listed in Table S2.

Strains and Growth Conditions. The wild-type *P. aeruginosa* PAO1, attenuated strain ExoST, and the pys2 and imm_{S2} gene double-knockout mutant strain, ΔS2i, were all from our laboratory. *E. coli* strains TOP10 and BL21 (DE3) were used for plasmid construction and protein purification, respectively. Unless stated elsewhere, both *E. coli* and *P. aeruginosa* strains were grown in LB broth or on LB agar at 37 °C without light. When required, antibiotics were added to the medium at the following concentrations (μg/mL): gentamicin, 15; kanamycin, 30 (*E. coli*); gentamicin, 30 (*P. aeruginosa*).

Plasmid Construction. The pys2 and imm_{S2} gene fragments were amplified by the polymerase chain reaction (PCR) from the wild-type *P. aeruginosa* PAO1 genome. Colicin E3 and its immune protein gene sequences were derived from the *E. coli* plasmid pColE3-CA38, and their gene fragments were synthetic (Sangon Biotech, China). The chimeric pyocin ChPy gene fragment was obtained by overlapping PCR of the gene blocks from pyocin S2 (1−1674 bp) and colicin E3 (1350−1656 bp).[14,30] All plasmids were constructed via Gibson assembly and transformed into TOP10 chemically competent *E. coli*. The plasmids were confirmed via Sanger sequencing before transformation into *P. aeruginosa* strains or the *E. coli* strain BL21 (DE3).

Purification of Pyocin S2 and Chimeric Pyocin ChPy. The purification of His_6-tagged pyocin complexes by Ni-NTA affinity chromatography was the same as in the previous article.[57] Briefly, 2 mL overnight cultures of S2-Imm_{S2}-pET28a-BL21 (DE3) and ChPy-Imm_{E3}-pET28a-BL21 (DE3) were transferred into 200 mL of fresh LB broth and were then incubated until the prelog phase was reached (OD_{600} ≈ 0.2−0.3). Protein overexpression was induced with 1 mM isopropyl-β-D-thiogalactopyranoside, and cultures were incubated with shaking at 200 rpm at 16 °C for an additional 20 h. *E. coli* cells were harvested through centrifugation (5000 rpm, 10 min) and resuspended in TGE buffer (50 mM Tris−HCl (pH 7.5), 1 mM EDTA, 10% glycerol, and 10 mM imidazoles) and disrupted via pulsed sonication. The cell debris was removed by centrifugation at 8000 rpm for 30 min at 4 °C. The supernatant was loaded onto a Hi-Trap FF column (Amersham Biosciences, GE Healthcare) integrated by an AKTA TM FPLC system (Amersham Biosciences, GE Healthcare). The His_6-tagged proteins were eluted using the elution buffer (1 M imidazole in 20 mM Tris−HCl (pH 7.5)). The purity of the His_6-tagged proteins was examined by Precast-GLgel Hepes SDS-PAGE 4−15% (Sangon, Biotech, China). The purified proteins were dialyzed against dialysis buffer (20 mM Tris−HCl (pH 7.5) and 150 mM NaCl). The protein concentration was determined using a BCA protein assay kit (Thermo Fisher Scientific, USA). The final pooled pure proteins were divided into several 1.5 mL tubes at −20 °C and thawed individually at 4 °C before each manipulation.

Pyocin S2 and ChPy Antimicrobial Activity Evaluation in FAB Agar. The OD_{600} values of overnight cultures of PAO1 and ΔS2i strains were unified to 0.3 using minimal medium FAB containing 1 mM $FeCl_3$ and 30 mM glutamate (FAB^{++}).[58] Subsequently, they were mixed with preheated 1.5% FAB^{++} agar at 65 °C in a 1:25 ratio by volume. Then, the mixed components were poured onto plates of 6 cm diameter (∼10 mL/plate) and allowed to solidify at room temperature

https://doi.org/10.1021/acssynbio.2c00655
ACS Synth. Biol. XXXX, XXX, XXX−XXX

for 25 min. Plates made in this way were named PAO1 and ΔS2i plates, respectively. Also, 2.5 μL pure protein complexes (0.158 mg/mL), $S2^{+I}$ and $ChPy^{+I}$, were spotted on PAO1 and ΔS2i plates, respectively. Finally, they were incubated overnight at 30 °C, and the diameter of pyocin inhibition zones was observed.

Pyocin S2 and ChPy Antimicrobial Activity Evaluation in Liquid Culture. The OD_{600} values of PAO1 and ΔS2i strains were unified using the method described above and then diluted at 1:100 by volume with FAB^{++} medium. The concentrations of the protein complexes, $S2^{+I}$ and $ChPy^{+I}$, were homogenized to 0.158 mg/mL. Subsequently, they and the dialysis buffer (control) were mixed with diluted PAO1 and ΔS2i cultures at a volume ratio of 1:3.5. Finally, 180 μL of mixed culture was pipetted into 96-well plates, and OD_{600} values were measured every 20 min using a Synergy HT microplate reader (BioTek) at 30 °C.

Swimming Assays. To prepare the semisolid agar motility plates, we poured 0.25% FAB^{+++}agar (FAB containing 1 mM $FeCl_3$, 30 mM glutamate, and 30 μg/mL gentamicin) at 65 °C into dishes with a diameter of 9 (~25 mL/plate) or 6 cm (~10 mL/plate) and allowed them to solidify at room temperature for 25 min. Subsequently, 750 μL of strains $PAO1^g$, $\Delta S2i^g$, PC100, Q017, and C100 with OD_{600} values unified to 0.8 was collected separately, and the pellet was resuspended in a 50 μL fresh FAB^{+++} medium. Finally, the 1.5 μL resuspension was stabbed into semisolid agar motility plates and cultured under light and dark conditions at 30 °C.

Semisolid Agar Antibacterial Analysis. The $PAO1^g$ and $\Delta S2i^g$ plates were prepared the same way as above. Briefly, strains $PAO1^g$ and $\Delta S2i^g$ (OD_{600} = 0.8) were mixed with 0.25% FAB^{+++} agar at 65 °C in a 1:200 ratio of volume. Then, 1.5 μL of the bacterial resuspension was stabbed into $PAO1^g$ or $\Delta S2i^g$ plates and cultured under light and dark conditions at 30 °C.

Strain C1028 Antimicrobial Activity Evaluation in Liquid Culture. The OD_{600} values of all strains were unified to 0.8 using FAB^{+++} medium, and the strains $PAO1^g$ and $\Delta S2i^g$ were mixed with C1028 and Q017 in volume ratios of 5:1, 3:1, 1:1, and 1:2. Finally, their OD_{600} values were monitored as before.

Mouse Wound Infection Model. The operational procedures for our mouse model were established based on the work of Zhao et al.[59] Adult female BALB/c mice, 6−8 weeks old, were used. Before forming the wounds, the mice were anesthetized with intraperitoneal injections of 1% sodium pentobarbital (45 mg/kg), and their dorsal surfaces were later shaved. Skin wounds were made on the dorsal surfaces of mice using a disposable 10 mm skin biopsy punch one time on the back of each mouse after anesthesia. Mice were randomly divided into five groups: PBS, +PBS, +Q017,+C1028, and $+C1028^d$. Then, 50 μL of sterile PBS buffer was added to the wounds of mice in the PBS group and incubated for 30 min. For the other four groups of mice, the wounds were infected by a 50 μL bacterial suspension of PAO1 (OD_{600} = 0.35) and incubated for 30 min. Then, 50 μL of PBS buffer and the bacterial suspension of Q017 and C1028 (OD_{600} = 0.7) was added to the wounds of mice in the +PBS, +Q017,+C1028, and $+C1028^d$ groups. The wounds of the mice were covered with Tegaderm (3 M) 30 min later to prevent contamination. The $+C1028^d$ group of mice needed to be incubated away from light, while the other four groups of mice were raised under 650 nm red light (1.2 mW/cm^2), and the wound area and body weight of the mice were counted daily. After 15 days, all the mice were killed by cervical dislocation. The culture and suspension preparation of all engineered strains were performed under dark conditions before application to wounds.

All animals received humane care, and experimental protocols were conducted following the Guide for the Care and Use of Laboratory Animals of the University of Science and Technology of China, as approved by the Animal Care Committee of Anhui Province (USTCACUC202001046).

CFU Counting. Skins and subcutaneous tissues (1 cm in diameter) from the wound centers of mice in the C1028, +PBS, and +C1028 groups were collected in 500 μL of sterile PBS buffer. Subsequently, the solution obtained after homogenizer treatment was serially diluted, applied to LB agar, and incubated for 12−16 h. CFU was determined using the standard CFU counting method.

■ ASSOCIATED CONTENT

Supporting Information

The Supporting Information is available free of charge at https://pubs.acs.org/doi/10.1021/acssynbio.2c00655.

Analysis of the targeted anti-*P. aeruginosa* effect of the pyocin complexes $S2^{+I}$ and $ChPy^{+I}$ (Figure S1); schematic diagram of the gene circuit of the host strain ExoST and the plasmid of the final system (Figure S2); evaluated effects of different NIR light intensities on motility and growth of engineered bacteria (Figure S3); optimization of the antibacterial ability of engineered bacteria (Figure S4); quantitative analysis of ChPy expression in several engineered bacteria (Figure S5); inhibition analysis of $PAO1^g$, $\Delta S2^g$, and $ExoST^g$ strains (Figure S6); safety analysis of engineered bacteria C1028 in the PAO1-infected mouse wound model (Figure S7); assessment of the therapeutic ability of the strain C1028 with or without light in the PAO1-infected mouse wound model (Figure S8); predicted strength and sequence of RBS used in this study (Table S1); bacterial strains and plasmids used in this study (Table S2) (PDF)

■ AUTHOR INFORMATION

Corresponding Authors

Fan Jin − *Hefei National Laboratory for Physical Sciences at the Microscale, University of Science and Technology of China, Hefei, Anhui 230026, P. R. China; CAS Key Laboratory of Quantitative Engineering Biology, Shenzhen Institute of Synthetic Biology, Shenzhen Institutes of Advanced Technology, Chinese Academy of Sciences, Shenzhen, Guangdong 518055, China;* orcid.org/0000-0003-2313-0388; Email: fan.jin@siat.ac.cn

Rongrong Zhang − *CAS Key Laboratory of Quantitative Engineering Biology, Shenzhen Institute of Synthetic Biology, Shenzhen Institutes of Advanced Technology, Chinese Academy of Sciences, Shenzhen, Guangdong 518055, China;* Email: rr.zhang@siat.ac.cn

Authors

Yanmei Gao − *Hefei National Laboratory for Physical Sciences at the Microscale, University of Science and Technology of China, Hefei, Anhui 230026, P. R. China; CAS Key Laboratory of Quantitative Engineering Biology,*

Shenzhen Institute of Synthetic Biology, Shenzhen Institutes of Advanced Technology, Chinese Academy of Sciences, Shenzhen, Guangdong 518055, China

Jingjing Wei − *Department of Fine Chemical Engineering, Shenzhen Polytechnic, Shenzhen, Guangdong 518055, China*

Lu Pu − *West China School of Medicine, West China Hospital of Sichuan University, Chengdu, Sichuan 610065, China*

Shengwei Fu − *Hefei National Laboratory for Physical Sciences at the Microscale, University of Science and Technology of China, Hefei, Anhui 230026, P. R. China*

Xiaochen Xing − *CAS Key Laboratory of Quantitative Engineering Biology, Shenzhen Institute of Synthetic Biology, Shenzhen Institutes of Advanced Technology, Chinese Academy of Sciences, Shenzhen, Guangdong 518055, China*

Complete contact information is available at: https://pubs.acs.org/10.1021/acssynbio.2c00655

Author Contributions

⊥Y.G. and J.W. contributed equally to this work.

Author Contributions

F.J. and Y.G. designed the experiments. Y.G., R.Z., L.P., and S.F. performed experiments. Y.G., J.W., X.X., and F.J. are responsible for data interpretation and manuscript preparation. All authors reviewed the manuscript.

Funding

This work was supported by the National Key Research and Development Program of China (2018YFA0902700), the National Natural Science Foundation of China (32000061), the China Postdoctoral Science Foundation (BX201700227), the Scientific Instrument Developing Project of the Chinese Academy of Sciences (Grant No. YJKYYQ20200033), the Chang'an Capital (ArtB Project), and the Shenzhen Engineering Research Center of Therapeutic Synthetic Microbes XMHT20220104015 (F.J.).

Notes

The authors declare no competing financial interest.

■ ACKNOWLEDGMENTS

We thank J.D. Shrout for providing the PAO1 strain and Shenzhen Synthetic Biology Infrastructure.

■ ABBREVIATIONS

NIR, near-infrared; AMPs, antimicrobial peptides; QS, quorum sensing; AHL, acyl-homoserine lactones; PI, propidium iodide; sfGFP, superfolder green fluorescent protein; RBSs, ribosome-binding sites; CFU, colony-forming unit; MDR, multidrug resistant

■ REFERENCES

(1) Pachori, P.; Gothalwal, R.; Gandhi, P. Emergence of antibiotic resistance *Pseudomonas aeruginosa* in intensive care unit; a critical review. *Genes Dis.* **2019**, *6*, 109−119.

(2) Fanelli, U.; Chiné, V.; Pappalardo, M.; Gismondi, P.; Esposito, S. Improving the Quality of Hospital Antibiotic Use: Impact on Multidrug-Resistant Bacterial Infections in Children. *Front. Pharmacol.* **2020**, *11*, 745.

(3) Affhan, S.; Dachang, W.; Xin, Y.; Shang, D. Lactic acid bacteria protect human intestinal epithelial cells from Staphylococcus aureus and *Pseudomonas aeruginosa* infections. *Genet. Mol. Res.* **2015**, *14*, 17044−17058.

(4) Annunziato, G.; Costantino, G. Antimicrobial peptides (AMPs): a patent review (2015-2020). *Expert Opin. Ther. Pat.* **2020**, 931.

(5) Six, A.; Mosbahi, K.; Barge, M.; Kleanthous, C.; Evans, T.; Walker, D. Pyocin efficacy in a murine model of *Pseudomonas aeruginosa* sepsis. *J. Antimicrob. Chemother.* **2021**, *76*, 2317−2324.

(6) Armijo, L. M.; Wawrzyniec, S. J.; Kopciuch, M.; Brandt, Y. I.; Rivera, A. C.; Withers, N. J.; Cook, N. C.; Huber, D. L.; Monson, T. C.; Smyth, H. D. C.; et al. Antibacterial activity of iron oxide, iron nitride, and tobramycin conjugated nanoparticles against *Pseudomonas aeruginosa* biofilms. *J. Nanobiotechnol.* **2020**, *18*, 35.

(7) Sánchez-López, E.; Gomes, D.; Esteruelas, G.; Bonilla, L.; Lopez-Machado, A. L.; Galindo, R.; Cano, A.; Espina, M.; Ettcheto, M.; Camins, A.; et al. Metal-Based Nanoparticles as Antimicrobial Agents: An Overview. *Nanomaterials* **2020**, *10*, 292.

(8) Pang, Z.; Raudonis, R.; Glick, B. R.; Lin, T. J.; Cheng, Z. Antibiotic resistance in *Pseudomonas aeruginosa*: mechanisms and alternative therapeutic strategies. *Biotechnol. Adv.* **2019**, *37*, 177−192.

(9) Behrens, H. M.; Six, A.; Walker, D.; Kleanthous, C. The therapeutic potential of bacteriocins as protein antibiotics. *Emerging Top. Life Sci.* **2017**, *1*, 65−74.

(10) Ling, H.; Saeidi, N.; Rasouliha, B. H.; Chang, M. W. A predicted S-type pyocin shows a bactericidal activity against clinical *Pseudomonas aeruginosa* isolates through membrane damage. *FEBS Lett.* **2010**, *584*, 3354−3358.

(11) McCaughey, L. C.; Ritchie, N. D.; Douce, G. R.; Evans, T. J.; Walker, D. Efficacy of species-specific protein antibiotics in a murine model of acute *Pseudomonas aeruginosa* lung infection. *Sci. Rep.* **2016**, *6*, 30201.

(12) Redero, M.; Aznar, J.; Prieto, A. I. Antibacterial efficacy of R-type pyocins against *Pseudomonas aeruginosa* on biofilms and in a murine model of acute lung infection. *J. Antimicrob. Chemother.* **2020**, *75*, 2188−2196.

(13) Heselpoth, R. D.; Euler, C. W.; Schuch, R.; Fischetti, V. A. Lysocins: Bioengineered Antimicrobials That Deliver Lysins across the Outer Membrane of Gram-Negative Bacteria. *Antimicrob. Agents Chemother.* **2019**, *63*, e00342−e00319.

(14) Gupta, S.; Bram, E. E.; Weiss, R. Genetically programmable pathogen sense and destroy. *ACS Synth. Biol.* **2013**, *2*, 715−723.

(15) Paškevičius, S.; Dapkutė, V.; Misiūnas, A.; Balzaris, M.; Thommes, P.; Sattar, A.; Gleba, Y.; Ražanskienė, A. Chimeric bacteriocin S5-PmnH engineered by domain swapping efficiently controls *Pseudomonas aeruginosa* infection in murine keratitis and lung models. *Sci. Rep.* **2022**, *12*, 5865.

(16) Kageyama, M.; Kobayashi, M.; Sano, Y.; Masaki, H. Construction and characterization of pyocin-colicin chimeric proteins. *J. Bacteriol.* **1996**, *178*, 103−110.

(17) Kang, M.; Choe, D.; Kim, K.; Cho, B. K.; Cho, S. Synthetic Biology Approaches in The Development of Engineered Therapeutic Microbes. *Int. J. Mol. Sci.* **2020**, *21*, 8744.

(18) Mao, N.; Cubillos-Ruiz, A.; Cameron, D. E.; Collins, J. J. Probiotic strains detect and suppress cholera in mice. *Sci. Transl. Med.* **2018**, *10*, No. eaao2586.

(19) Saeidi, N.; Wong, C. K.; Lo, T. M.; Nguyen, H. X.; Ling, H.; Leong, S. S.; Poh, C. L.; Chang, M. W. Engineering microbes to sense and eradicate *Pseudomonas aeruginosa*, a human pathogen. *Mol. Syst. Biol.* **2011**, *7*, 521.

(20) Palmer, J. D.; Piattelli, E.; McCormick, B. A.; Silby, M. W.; Brigham, C. J.; Bucci, V. Engineered Probiotic for the Inhibition of Salmonella via Tetrathionate-Induced Production of Microcin H47. *ACS Infect. Dis.* **2018**, *4*, 39−45.

(21) Hwang, I. Y.; Koh, E.; Wong, A.; March, J. C.; Bentley, W. E.; Lee, Y. S.; Chang, M. W. Engineered probiotic Escherichia coli can eliminate and prevent *Pseudomonas aeruginosa* gut infection in animal models. *Nat. Commun.* **2017**, *8*, 1−11.

(22) Hwang, I. Y.; Tan, M. H.; Koh, E.; Ho, C. L.; Poh, C. L.; Chang, M. W. Reprogramming microbes to be pathogen-seeking killers. *ACS Synth. Biol.* **2014**, *3*, 228−237.

(23) Riglar, D. T.; Silver, P. A. Engineering bacteria for diagnostic and therapeutic applications. *Nat. Rev. Microbiol.* **2018**, *16*, 214−225.

(24) Stephens, K.; Bentley, W. E. Synthetic Biology for Manipulating Quorum Sensing in Microbial Consortia. *Trends Microbiol.* **2020**, *28*, 633−643.
(25) Baumschlager, A.; Khammash, M. Synthetic Biological Approaches for Optogenetics and Tools for Transcriptional Light-Control in Bacteria. *Adv. Biol.* **2021**, *5*, No. e2000256.
(26) Mazraeh, D.; Di Ventura, B. Synthetic microbiology applications powered by light. *Curr. Opin. Microbiol.* **2022**, *68*, No. 102158.
(27) Wang, S.; Zhang, Z.; Wei, S.; He, F.; Li, Z.; Wang, H. H.; Huang, Y.; Nie, Z. Near-infrared light-controllable MXene hydrogel for tunable on-demand release of therapeutic proteins. *Acta Biomater.* **2021**, *130*, 138−148.
(28) Ryu, M. H.; Gomelsky, M. Near-infrared light responsive synthetic c-di-GMP module for optogenetic applications. *ACS Synth. Biol.* **2014**, *3*, 802−810.
(29) Smith, K.; Martin, L.; Rinaldi, A.; Rajendran, R.; Ramage, G.; Walker, D. Activity of pyocin S2 against *Pseudomonas aeruginosa* biofilms. *Antimicrob. Agents Chemother.* **2012**, *56*, 1599−1601.
(30) Michel-Briand, Y.; Baysse, C. The pyocins of *Pseudomonas aeruginosa*. *Biochimie* **2002**, *84*, 499−510.
(31) White, P.; Joshi, A.; Rassam, P.; Housden, N. G.; Kaminska, R.; Goult, J. D.; Redfield, C.; McCaughey, L. C.; Walker, D.; Mohammed, S.; et al. Exploitation of an iron transporter for bacterial protein antibiotic import. *Proc. Natl. Acad. Sci.* **2017**, *114*, 12051−12056.
(32) McCaughey, L. C.; Josts, I.; Grinter, R.; White, P.; Byron, O.; Tucker, N. P.; Matthews, J. M.; Kleanthous, C.; Whitchurch, C. B.; Walker, D. Discovery, characterization and in vivo activity of pyocin SD2, a protein antibiotic from *Pseudomonas aeruginosa*. *Biochem. J.* **2016**, *473*, 2345−2358.
(33) Behrens, H. M.; Lowe, E. D.; Gault, J.; Housden, N. G.; Kaminska, R.; Weber, T. M.; Thompson, C. M. A.; Mislin, G. L. A.; Schalk, I. J.; Walker, D.; et al. Pyocin S5 Import into *Pseudomonas aeruginosa* Reveals a Generic Mode of Bacteriocin Transport. *MBio* **2020**, *11*, No. e03230-19.
(34) Soelaiman, S.; Jakes, K.; Wu, N.; Li, C.; Shoham, M. Crystal Structure of Colicin E3. *Mol. Cell* **2001**, *8*, 1053−1062.
(35) Fu, S.; Zhang, R.; Gao, Y.; Xiong, J.; Li, Y.; Pu, L.; Xia, A.; Jin, F. Programming the lifestyles of engineered bacteria for cancer therapy. *Nat. Sci. Rev.* **2023**, *10*, nwad031.
(36) Deighan, P.; Hochschild, A. The bacteriophage lambdaQ anti-terminator protein regulates late gene expression as a stable component of the transcription elongation complex. *Mol. Microbiol.* **2007**, *63*, 911−920.
(37) Bhasme, P.; Wei, Q.; Xu, A.; Naqvi, S. T. A.; Wang, D.; Ma, L. Z. Evaluation and characterization of the predicted diguanylate cyclase-encoding genes in *Pseudomonas aeruginosa*. *Microbiology* **2020**, *9*, No. e975.
(38) Mori, Y.; Yoshida, Y.; Satoh, A.; Moriya, H. Development of an experimental method of systematically estimating protein expression limits in HEK293 cells. *Sci. Rep.* **2020**, *10*, 4798.
(39) Hui, C. Y.; Guo, Y.; Zhang, W.; Huang, X. Q. Rapid monitoring of the target protein expression with a fluorescent signal based on a dicistronic construct in Escherichia coli. *AMB Express* **2018**, *8*, 81.
(40) Salis, H. M. The ribosome binding site calculator. *Methods Enzymol.* **2011**, *498*, 19−42.
(41) Turnbull, L.; Toyofuku, M.; Hynen, A. L.; Kurosawa, M.; Pessi, G.; Petty, N. K.; Osvath, S. R.; Cárcamo-Oyarce, G.; Gloag, E. S.; Shimoni, R.; et al. Explosive cell lysis as a mechanism for the biogenesis of bacterial membrane vesicles and biofilms. *Nat. Commun.* **2016**, *7*, 11220.
(42) Penterman, J.; Singh, P. K.; Walker, G. C. Biological cost of pyocin production during the SOS response in *Pseudomonas aeruginosa*. *J. Bacteriol.* **2014**, *196*, 3351−3359.
(43) Chen, F.; Chen, G.; Liu, Y.; Jin, Y.; Cheng, Z.; Liu, Y.; Yang, L.; Jin, S.; Wu, W. *Pseudomonas aeruginosa* Oligoribonuclease Contributes to Tolerance to Ciprofloxacin by Regulating Pyocin Biosynthesis. *Antimicrob. Agents Chemother.* **2017**, *61*, e02256−e02216.
(44) Jones, S. G.; Edwards, R.; Thomas, D. W. Inflammation and wound healing: the role of bacteria in the immuno-regulation of wound healing. *Int. J. Lower Extremity Wounds* **2004**, *3*, 201−208.
(45) Gut, A. M.; Vasiljevic, T.; Yeager, T.; Donkor, O. N. Salmonella infection-prevention and treatment by antibiotics and probiotic yeasts: a review. *Microbiology* **2018**, *164*, 1327−1344.
(46) Pacheco, T.; Bustos-Cruz, R. H.; Abril, D.; Arias, S.; Uribe, L.; Rincón, J.; García, J. C.; Escobar-Perez, J. *Pseudomonas aeruginosa* Coharboring BlaKPC-2 and BlaVIM-2 Carbapenemase Genes. *Antibiotics* **2019**, *8*, 98.
(47) Denayer, S.; Matthijs, S.; Cornelis, P. Pyocin S2 (Sa) kills *Pseudomonas aeruginosa* strains via the FpvA type I ferripyoverdine receptor. *J. Bacteriol.* **2007**, *189*, 7663−7668.
(48) Liu, N.; Lewis, C.; Zheng, W.; Fu, Z. Q. Phage Cocktail Therapy: Multiple Ways to Suppress Pathogenicity. *Trends Plant Sci.* **2020**, *25*, 315−317.
(49) Adepu, S.; Ramakrishna, S. Controlled Drug Delivery Systems: Current Status and Future Directions. *Molecules* **2021**, *26*, 5905.
(50) Pollard, A. J.; Bijker, E. M. A guide to vaccinology: from basic principles to new developments. *Nat. Rev. Immunol.* **2021**, *21*, 83−100.
(51) Dróżdż, M.; Makuch, S.; Cieniuch, G.; Woźniak, M.; Ziółkowski, P. Obligate and facultative anaerobic bacteria in targeted cancer therapy: Current strategies and clinical applications. *Life Sci.* **2020**, *261*, No. 118296.
(52) Huang, X.; Pan, J.; Xu, F.; Shao, B.; Wang, Y.; Guo, X.; Zhou, S. Bacteria-Based Cancer Immunotherapy. *Advanced. Science* **2021**, *8*, No. 2003572.
(53) Felgner, S.; Kocijancic, D.; Frahm, M.; Curtiss, R., 3rd; Erhardt, M.; Weiss, S. Optimizing Salmonella enterica serovar Typhimurium for bacteria-mediated tumor therapy. *Gut Microbes* **2016**, *7*, 171−177.
(54) Milligan, R.; Paul, M.; Richardson, M.; Neuberger, A. Vaccines for preventing typhoid fever. *Cochrane Database Syst. Rev.* **2018**, *5*, No. CD001261.
(55) Healing Societies (WUWHS). Wound infection in clinical practice. An international consensus. *Int. Wound J.* **2008**, *5*, iii−11.
(56) Wilhelm, K. P.; Wilhelm, D.; Bielfeldt, S. Models of wound healing: an emphasis on clinical studies. *Skin Res. Technol.* **2017**, *23*, 3−12.
(57) Elfarash, A.; Wei, Q.; Cornelis, P. The soluble pyocins S2 and S4 from *Pseudomonas aeruginosa* bind to the same FpvAI receptor. *Microbiology* **2012**, *1*, 268−275.
(58) Pu, L.; Yang, S.; Xia, A.; Jin, F. Optogenetics Manipulation Enables Prevention of Biofilm Formation of Engineered *Pseudomonas aeruginosa* on Surfaces. *ACS Synth. Biol.* **2018**, *7*, 200−208.
(59) Zhao, Z. J.; Xu, Z. P.; Ma, Y. Y.; Ma, J. D.; Hong, G. Photodynamic antimicrobial chemotherapy in mice with *Pseudomonas aeruginosa*-infected wounds. *PLoS One* **2020**, *15*, No. e0237851.

https://doi.org/10.1021/acssynbio.2c00655
ACS Synth. Biol. XXXX, XXX, XXX−XXX